5-2019

Disruption of valosin-containing protein activity causes cardiomyopathy and reveals pleiotropic functions in cardiac homeostasis

Matthew J. Brody
University of Cincinnati

Davy Vanhoutte
University of Cincinnati

Chinmay V. Bakshi
University of Cincinnati

Ruijie Liu
Grand Valley State University, liuruiji@gvsu.edu

Robert N. Correll
University of Cincinnati

See next page for additional authors

JBC ARTICLE

Disruption of valosin-containing protein activity causes cardiomyopathy and reveals pleiotropic functions in cardiac homeostasis

Received for publication, January 16, 2019, and in revised form, April 8, 2019 Published, Papers in Press, April 21, 2019, DOI 10.1074/jbc.RA119.007585

Matthew J. Brody[‡], Davy Vanhoutte[‡], Chinmay V. Bakshi[‡], Ruije Liu[‡§], Robert N. Correll[‡¶], Michelle A. Sargent[‡], and Jeffery D. Molkentin[‡‖1]

From the [‡]Department of Pediatrics, Cincinnati Children's Hospital Medical Center, University of Cincinnati, Cincinnati, Ohio 45229-3039, the [‖]Howard Hughes Medical Institute, Cincinnati, Ohio 45229-3039, the [§]Department of Biomedical Sciences, Grand Valley State University, Allendale, Michigan 49401, and the [¶]Department of Biological Sciences, University of Alabama, Tuscaloosa, Alabama 35487-0344

Edited by George N. DeMartino

Valosin-containing protein (VCP), also known as p97, is an ATPase with diverse cellular functions, although the most highly characterized is targeting of misfolded or aggregated proteins to degradation pathways, including the endoplasmic reticulum–associated degradation (ERAD) pathway. However, how VCP functions in the heart has not been carefully examined despite the fact that human mutations in VCP cause Paget disease of bone and frontotemporal dementia, an autosomal dominant multisystem proteinopathy that includes disease in the heart, skeletal muscle, brain, and bone. Here we generated heart-specific transgenic mice overexpressing WT VCP or a VCP^{K524A} mutant with deficient ATPase activity. Transgenic mice overexpressing WT VCP exhibit normal cardiac structure and function, whereas mutant VCP-overexpressing mice develop cardiomyopathy. Mechanistically, mutant VCP-overexpressing hearts up-regulate ERAD complex components and have elevated levels of ubiquitinated proteins prior to manifestation of cardiomyopathy, suggesting dysregulation of ERAD and inefficient clearance of proteins targeted for proteasomal degradation. The hearts of mutant VCP transgenic mice also exhibit profound defects in cardiomyocyte nuclear morphology with increased nuclear envelope proteins and nuclear lamins. Proteomics revealed overwhelming interactions of endogenous VCP with ribosomal, ribosome-associated, and RNA-binding proteins in the heart, and impairment of cardiac VCP activity resulted in aggregation of large ribosomal subunit proteins. These data identify multifactorial functions and diverse mechanisms whereby VCP regulates cardiomyocyte protein and RNA quality control that are critical for cardiac homeostasis, suggesting how human *VCP* mutations negatively affect the heart.

Mutations in valosin-containing protein (VCP, [2] also known as p97, the mammalian homologue of yeast Cdc48) are the cause of inclusion body myopathy associated with Paget disease of bone and frontotemporal dementia (IBMPFD), a degenerative multisystem proteinopathy that causes pathology of the skeletal muscle, brain, bone, and heart. IBMPFD is characterized by progressive muscle weakness that presents in adulthood and can ultimately include heart failure, dementia, and abnormal bone growth (1–4). VCP forms a barrel-shaped homohexamer that functions as an ATPase through the action of its D1 and D2 domains, whereas its N-terminal domain recruits VCP to different subcellular locations (5–10). VCP has been ascribed an array of cellular functions, including protein quality control (7, 11–16), membrane fusion (17), chromatin remodeling (18), disassembly of the DNA helicase complex (19, 20), DNA repair (21), formation of the endoplasmic reticulum (ER) (22) and nuclear envelope (23), and regulation of RNA stability (24). However, the best-characterized molecular function for VCP is providing energy to extract terminally misfolded polypeptides from the ER into the cytosol for degradation by the ubiquitin proteasome system (UPS) in a process termed ER-associated degradation (ERAD) (7, 11–14, 16). VCP additionally functions in nuclear protein quality control in a pathway analogous to ERAD at the inner nuclear membrane (INM) (25, 26).

VCP also directly associates with the large ribosomal subunit (27–29) and functions in ribosome-associated degradation in yeast to release aberrant translated polypeptides from ribosomes for proteasomal degradation (27, 28, 30). A large portion of cellular energy is expended to assemble, maintain, turnover, and degrade the upwards of 10 million ribosomes present in a mammalian cell, which requires the action of diverse nonribo-

This work was supported by NIH grants F32HL124698 and K99HL136695 (to M. J. B.) and R01HL105924 (to J. D. M.) and grants from the Howard Hughes Medical Institute. The authors declare that they have no conflicts of interest with the contents of this article. The content is solely the responsibility of the authors and does not necessarily represent the official views of the National Institutes of Health.

This article contains Figs. S1–S4 and Table S1.

[1] To whom correspondence should be addressed: Dept. of Pediatrics, Cincinnati Children's Hospital Medical Center of the University of Cincinnati and the Howard Hughes Medical Institute, 240 Albert Sabin Way, MLC7020, Cincinnati OH 45229-3039. Tel.: 513-636-3557; Fax: 513-636-5958; E-mail: Jeff.Molkentin@cchmc.org.

[2] The abbreviations used are: VCP, valosin-containing protein; IBMPFD, inclusion body myopathy associated with Paget disease of bone and frontotemporal dementia; ER, endoplasmic reticulum; UPS, ubiquitin proteasome system; ERAD, endoplasmic reticulum–associated degradation; INM, inner nuclear membrane; RBP, RNA-binding protein; tTA, tetracycline transactivator; α-MHC, α-myosin heavy chain; DTg, double-transgenic; TAC, transverse aortic constriction; PERK, protein kinase R–like ER kinase; RNP, ribonucleoprotein; hnRNP, heterogeneous nuclear ribonucleoprotein; NPM, nucleophosmin; Y2H, yeast two-hybrid; cDNA, complementary DNA; IHC, immunohistochemistry; qPCR, quantitative real-time PCR; ANOVA, analysis of variance.

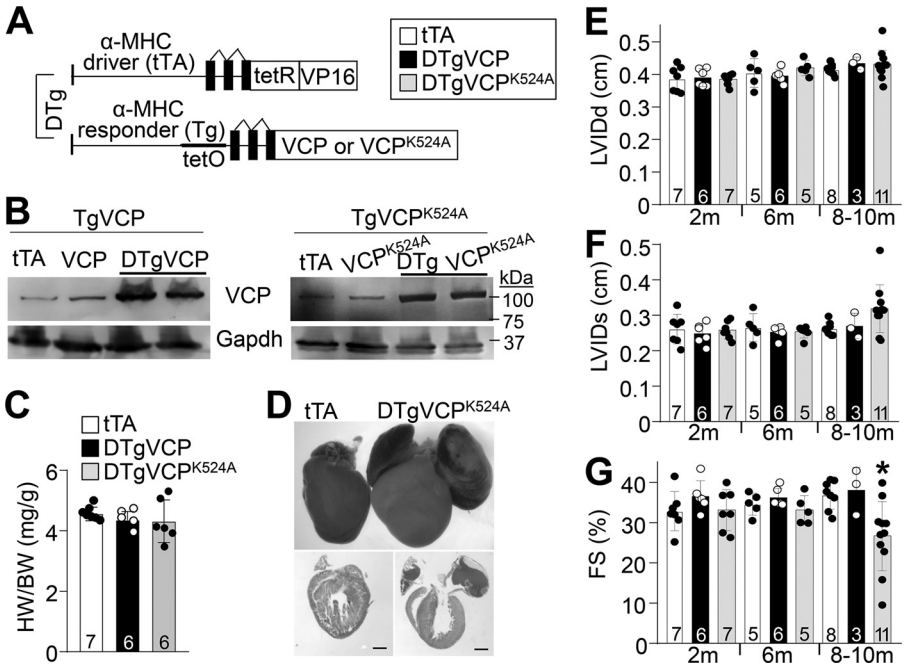

Figure 1. Impairment of cardiomyocyte VCP activity causes cardiomyopathy. *A*, schematic of the binary transgenic system used to induce heart-specific expression of WT VCP or an ATPase-deficient VCP mutant (VCP^{K524A}). *B*, Western blot of cardiac lysates for VCP in DTg mice overexpressing WT or K524A mutant VCP and single transgenic controls at 2 months of age. GAPDH was used as a sample processing and loading control. *C*, heart weight-to-body weight ratios at 6 months of age in the indicated genotypes of mice. *D*, gross morphology (*top*) and histology (H&E, *bottom*) of DTgVCP^{K524A} and tTA control hearts at 9 months of age. *Scale bars* = 1 mm. *E–G*, cardiac structure and function were evaluated at various ages in the indicated groups of mice by echocardiography to measure left ventricular inner chamber dimension in diastole (*LVIDd*, *E*), left ventricular inner chamber diameter in systole (*LVIDs*, *F*), and fractional shortening percentage (*FS*%, *G*) in mouse hearts at the indicated age in months. The number of mice analyzed is shown in the *columns* in *C* and *E–G*. *, $p < 0.05$ compared with tTA controls using one-way ANOVA with Tukey's post hoc test.

somal proteins, including many ATPases, RNA helicases, and RNA-binding proteins (RBPs) (31–33). However, specific functions for VCP in these processes have not been established.

VCP is abundantly expressed in the heart (34), and IBMPFD includes cardiomyopathy and heart failure (1–4). However, the pathways and processes that are regulated by VCP in cardiomyocytes are not known. To address this, we generated heart-specific transgenic mice overexpressing WT VCP or a VCP mutant with impaired ATPase activity (VCP^{K524A}) (8). Although overexpression of WT VCP is without noticeable effect, transgenic VCP^{K524A} mice develop cardiomyopathy, upregulate the ERAD machinery, and accumulate ubiquitinated proteins in the heart. Moreover, cardiomyocyte nuclear morphology is disrupted in VCP^{K524A}-overexpressing hearts, suggesting roles of VCP in maintaining the integrity of cardiomyocyte nuclei. Surprisingly, proteomics identified predominant interactions of VCP with ribosomal proteins, ribosome-associated proteins, and RBPs. Further investigation revealed accumulation and aggregation of large ribosomal subunit proteins in VCP-mutant hearts, suggesting underappreciated functions of VCP in ribostasis that may also contribute to IBMPFD in humans. Taken together, we have uncovered multiple protein and RNA quality control pathways through which VCP functions in cardiomyocytes to maintain cardiac homeostasis.

Results

Inhibition of VCP activity in cardiomyocytes causes cardiomyopathy

To investigate the cardiac functions of VCP, we generated transgenic mice with cardiomyocyte-specific overexpression of VCP. We utilized a bigenic transgene system that requires expression of both the tetracycline transactivator (tTA) transgene and the VCP transgene that contains the tetracycline operator within the α-myosin heavy chain (α-MHC) promoter to produce tetracycline- or doxycycline-repressible expression in cardiomyocytes (35) (Fig. 1*A*). The presence of both transgenes is referred to as double-transgenic (DTg). In addition to transgenic mice overexpressing WT VCP, we generated transgenic mice overexpressing a VCP^{K524A} mutant (Fig. 1*A*) to interrogate the effects of impaired VCP activity in the heart. Mutation of lysine 524 within the D2 ATPase domain of VCP to alanine results in dramatically reduced ATPase activity and produces a dominant-negative mutant that is deficient in segregase and protein complex remodeling functions (8). As expected, the hearts of WT or mutant VCP DTg mice maintained on normal lab chow in the absence of tetracycline or doxycycline (the bigenic transgene system is fully induced) had significantly increased VCP protein expression (Fig. 1*B*). WT and K524A mutant VCP transgenic mice showed no cardiac hypertrophy at 6 months of age (Fig. 1*C*). However, analysis of gross morphology and histology at 9 months of age revealed cardiac enlargement and atrial dilation in DTgVCP^{K524A} mice but not the WT (Fig. 1*D*). Cardiac structure and function of transgenic mice were evaluated by echocardiography, demonstrating normal cardiac morphology and function in mice overexpressing WT or mutant VCP in the heart through 6 months of age (Fig. 1, *E–G*), but by 8–10 months of age, DTgVCP^{K524A} mice developed systolic dysfunction, whereas aged DTgVCP mice remained normal (Fig. 1, *F* and *G*). Cardiomyopathy in aged DTgVCP^{K524A} mice occurs in the absence of significant

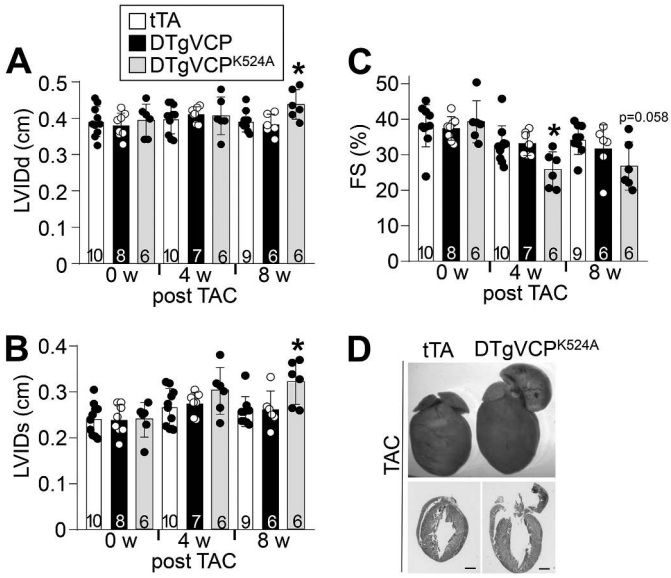

Figure 2. Exacerbated pressure overload-induced cardiac disease in mice with heart-specific overexpression of mutant VCP. *A–C*, cardiac left ventricular inner chamber dimension in diastole (*LVIDd*, *A*), left ventricular inner chamber diameter in systole (*LVIDs*, *B*), and fractional shortening percentage (*FS*%, *C*), evaluated by echocardiography in the indicated groups of mice 8–10 weeks of age without TAC (0 weeks) and 4 and 8 weeks after TAC surgery. The number of mice analyzed is shown in the columns. *, $p < 0.05$ compared with tTA controls at the same time point using one-way ANOVA with Tukey's post hoc test. *D*, heart gross morphology and histological analyses of cardiac sections stained with H&E from the indicated lines of mice 12 weeks after TAC surgery. *Scale bars* = 1 mm.

left ventricular hypertrophy or remodeling (Fig. 1, *C–G*, and Fig. S1, *A* and *B*). Thus, inhibition of VCP activity ultimately has a negative effect on cardiac function, suggesting important roles of VCP in cardiac homeostasis.

To further examine the pathologic effects of disrupting VCP ATPase activity in the heart, we performed transverse aortic constriction (TAC) to surgically induce pressure overload hypertrophy in VCP and VCP^{K524A} transgenic mice at 8–10 weeks of age. After 4 weeks of pressure overload, mice overexpressing VCP^{K524A} exhibited a substantial decline in cardiac function compared with tTA controls and mice with heart-specific overexpression of WT VCP (Fig. 2, *A–C*). By 8 weeks following TAC surgery, DTgVCP^{K524A} mice developed dilated cardiomyopathy, characterized by diminished cardiac functional performance, whereas tTA controls and DTgVCP mice did not undergo significant ventricular remodeling and had a relatively preserved cardiac functional response to pressure overload (Fig. 2, *A–C*). Histological evaluation confirmed ventricular dilation and revealed prominent dilation of the left atrium in DTgVCP^{K524A} mice (Fig. 2*D*), indicating increased sensitivity to pressure overload–induced cardiac dysfunction and remodeling when VCP ATPase activity is defective, compared with tTA control mice. Taken together, these data demonstrate that disruption of VCP ATPase activity causes age-dependent cardiomyopathy and hastens cardiac disease in response to pressure overload.

VCP activity is critical for cardiac proteostasis and ERAD

VCP underlies protein quality control, which commonly involves degradation of proteins by the UPS, including an indispensable role in the ERAD pathway, which removes misfolded proteins from the ER for UPS-mediated degradation in the cytoplasm (7, 11–14, 16). Hearts overexpressing VCP^{K524A} but not WT VCP had a significant elevation of ubiquitinated proteins in the soluble fraction (Fig. 3, *A* and *B*), indicating that inhibition of cardiac VCP activity results in defective clearance of proteins targeted for degradation by the UPS. Importantly, the accumulation of ubiquitinated proteins in DTgVCP^{K524A} hearts (Fig. 3, *A* and *B*) preceded cardiomyopathy, suggesting that proteotoxicity contributes to disease caused by inhibition of VCP ATPase activity.

Next we evaluated the ERAD pathway in transgenic hearts with manipulated VCP activity given the build-up of ubiquitinated proteins in DTg mutant hearts (Fig. 3, *A* and *B*) and given the known importance of ERAD in cardiac physiology (36). We performed Western blotting for various components of the ERAD pathway and ER-resident chaperones involved in protein folding and quality control. Sel1L, an ER membrane–embedded adaptor required for the dislocation of improperly folded proteins in the ER for degradation by ERAD (37–40), was up-regulated in hearts overexpressing either VCP or VCP^{K524A} compared with tTA controls (Fig. 3, *C* and *D*), indicating that VCP overexpression stabilizes an ERAD complex at the cardiomyocyte ER membrane. Homocysteine-induced ER protein (Herp), another crucial ER membrane adaptor for ERAD (41), and OS-9, an ER luminal lectin that binds misfolded glycoproteins in the ER for recognition by the ERAD complex (41, 42), were up-regulated specifically in hearts overexpressing the VCP^{K524A} mutant (Fig. 3, *C* and *D*). Importantly, the mRNA levels of the ERAD genes *Sel1L*, *OS9*, and *Herpud1* (encodes Herp) were not up-regulated, and some were even down-regulated in VCP mutant– overexpressing hearts (Fig. S2), indicating that the increased protein levels of ERAD factors observed in VCP-mutant hearts occurs through a posttranscriptional mechanism. These data suggest formation of additional ERAD protein complexes as a primary compensatory response to defective VCP activity and malfunctioning ERAD in the heart. These changes in expression of ERAD proteins occurred at 2 months of age (Fig. 3, *C* and *D*), before development of cardiomyopathy in DTgVCP^{K524A} mice. DTgVCP^{K524A} hearts also showed increased protein expression of the ER-resident prolyl isomerase cyclophilin B (CypB) (43) and protein disulfide isomerase (Fig. 3, *C* and *D*), both of which participate in targeting of substrates for ERAD (44–46). In contrast, expression of BiP and calnexin, ER chaperones that assist with folding of the bulk of secretory proteins in the ER (47), were unaltered (Fig. 3, *C* and *D*). Thus, impairment of VCP activity in the heart is associated with dysregulation of ERAD proteins and a build-up of ubiquitinated proteins.

To directly examine the effects of VCP inhibition on cardiomyocytes, we treated cultured rat neonatal cardiomyocytes with the VCP inhibitor DeBQ for 8 h, which resulted in a substantial accumulation of ubiquitinated proteins (Fig. 4, *A* and *B*). These data indicate that VCP activity is necessary for protein quality control and ubiquitin proteasome-mediated degradation and that acute inhibition of VCP disrupts cardiomyocyte proteostasis.

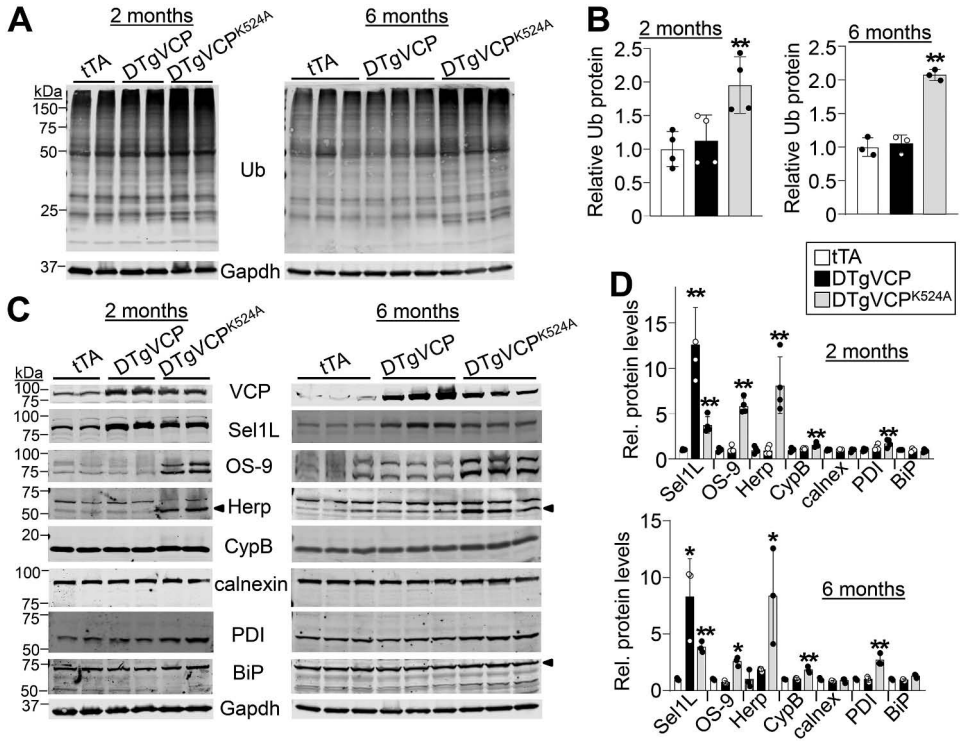

Figure 3. Dysregulation of ERAD and accumulation of ubiquitinated proteins in mutant VCP-overexpressing hearts. *A* and *B*, Western blot for total ubiquitinated (Ub) proteins in cardiac protein lysates at 2 and 6 months of age (*A*) and quantification of these levels in the indicated genotypes of mice at 2 and 6 months of age (*B*). $n = 4$ or 3 samples. *C* and *D*, Western blot (*C*) and quantitation (*D*) of the indicated endoplasmic reticulum and ERAD proteins in cardiac lysates at 2 and 6 months of age in the indicated genotypes of mice. $n = 4$ or 3 samples. **, $p < 0.01$; *, $p < 0.05$ compared with tTA controls using one-tailed Student's *t* test.

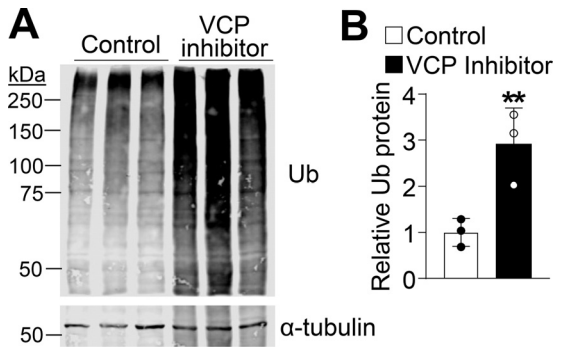

Figure 4. Acute inhibition of VCP disrupts cardiomyocyte proteostasis. *A* and *B*, Western blot (*A*) and quantification (*B*) of ubiquitinated (*Ub*) proteins in lysates of cultured neonatal rat cardiomyocytes treated with the VCP inhibitor DeBQ (5 μM for 8 h). α-tubulin is shown as a processing and loading control. **, $p < 0.01$ using one-tailed Student's *t* test.

The UPR is activated in response to ER stress and results in inhibition of translation and induction of expression of ER chaperones downstream of the three ER-membrane UPR sensors, activating transcription factor 6α (ATF6α), inositol-requiring enzyme 1α (IRE1α), and protein kinase R–like ER kinase (PERK) (48). The UPR thus serves as a parallel pathway to simultaneously enhance the protein folding capacity and reduce the protein folding load within the ER, whereas ERAD functions to remove terminally misfolded proteins from the ER for degradation by the UPS. Here we observed that VCP mutant hearts had increased levels of PERK and robust induction of the activated nuclear form of ATF6α (Fig. 5, *A* and *B*). VCP ATPase–deficient hearts did not exhibit activation of IRE1α or its downstream target Xbp1 (Fig. 5, *A* and *B*), indicating that the ATF6α and PERK branches of the UPR, but not the IRE1α pathway, are engaged in VCP mutant hearts, likely as a protective mechanism to cope with defective ERAD.

Disruption of VCP activity causes cardiomyocyte nuclear dysmorphology

To gain insight into cellular defects caused by disruption of cardiomyocyte VCP activity, we evaluated the subcellular architecture in transgenic hearts by transmission EM. The results demonstrated normal cardiomyocyte ultrastructure in single transgenic tTA control and DTgVCP hearts (Fig. 6*A*). Although cardiac ultrastructure was normal in all genotypes at 6 weeks of age (Fig. S3), by 5 months of age, which precedes the cardiomyopathy phenotype, hearts overexpressing the ATPase-deficient VCP mutant exhibit prominent defects in cardiomyocyte nuclear morphology, including abnormal nuclear shape, nuclear fragmentation, and increased invaginations in the nuclear membrane (Fig. 6*A*), suggesting that VCP activity is required to maintain nuclear structural integrity. These marked defects in nuclear morphology in DTgVCP^{K524A} hearts at 5 months of age were not accompanied by defects in myofilament or mitochondrial structure (Fig. 6*A*). We also performed EM at 10 months of age, when DTgVCP^{K524A} hearts are overtly diseased (Fig. 1), which revealed even more severe nuclear dysmorphology in DTgVCP^{K524A} cardiomyocytes, including the presence of intranuclear vesicles, intranuclear membraneless regions of low electron density, and mitochondrial ultrastructural abnormalities, whereas aged tTA control

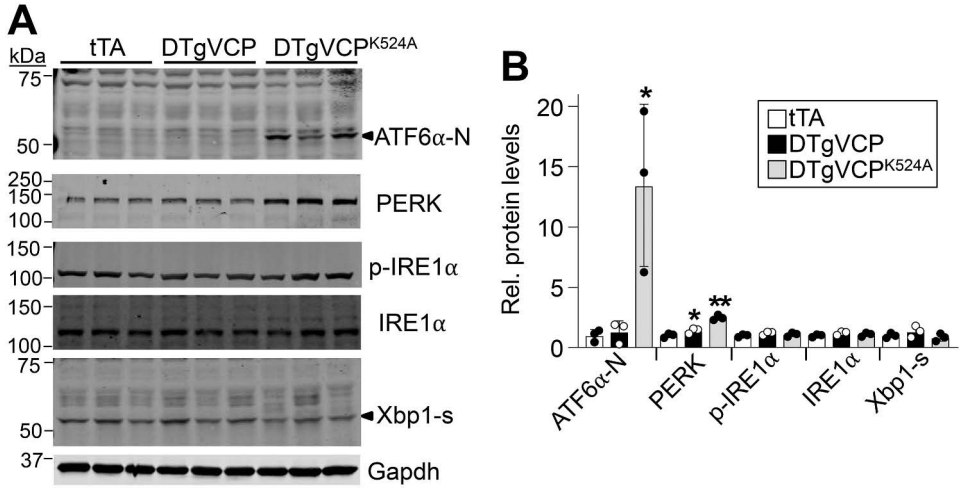

Figure 5. Activation of the UPR in VCP transgenic hearts. *A* and *B*, Western blot of components of the three branches of the UPR in cardiac protein lysates at 6 months of age (*A*) and quantification of protein levels (*B*) in the indicated genotypes of mice. Gapdh is shown as a processing and loading control. $n = 3$ samples for each genotype. **, $p < 0.01$; *, $p < 0.05$ compared with tTA controls using one-tailed Student's *t* test.

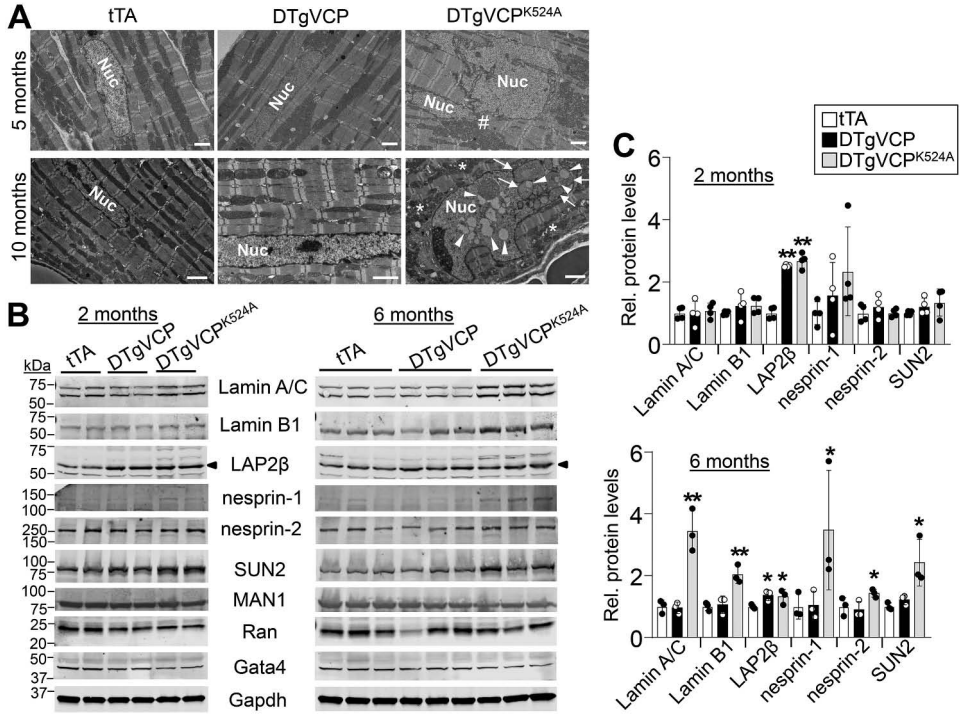

Figure 6. Cardiomyocyte nuclear dysmorphology in hearts with deficient VCP ATPase activity. *A*, transmission EM images of transgenic hearts of the indicated genotypes at 5 and 10 months of age. *Nuc*, nucleus. # indicates nuclear fragmentation. *Arrows* indicate intranuclear membrane-bound structures, and *arrowheads* point to intranuclear membraneless regions of low electron density. The *asterisk* denotes abnormal mitochondria. *Scale bars* = 2 μm. *B* and *C*, Western blot (*B*) and quantification (*C*) of nuclear membrane and nuclear lamina proteins using cardiac protein lysates from transgenic mice of the indicated genotypes at 2 and 6 months of age. Gapdh was used as a processing and loading control. $n = 4$ or 3 samples. **, $p < 0.01$; *, $p < 0.05$ compared with tTA controls using one-tailed Student's *t* test.

and DTgVCP hearts retained normal cardiomyocyte nuclear and subcellular ultrastructure (Fig. 6*A*).

To investigate molecular alterations that may underlie or coincide with the observed cardiomyocyte nuclear dysmorphology in DTgVCP^{K524A} hearts (Fig. 6*A*), we performed immunoblotting for nuclear lamins and components of the nuclear envelope and linker of nucleoskeleton and cytoskeleton complex in cardiac lysates from transgenic mice at 2 and 6 months of age. The results indicate an increased abundance of nuclear lamins and specific components of the nuclear envelope in hearts overexpressing the ATPase-deficient VCP mutant at 6 months of age (Fig. 6, *B* and *C*) prior to development of cardiomyopathy but following up-regulation of ERAD complex proteins (Fig. 3, *C* and *D*). Indeed, VCP^{K524A} hearts showed substantial up-regulation of lamin A/C as well as lamin B1, whereas the expression of nuclear lamins was unaltered by overexpression of WT VCP (Fig. 6, *B* and *C*). VCP^{K524A}-overexpressing hearts also had increased protein levels of the INM protein SUN2 and the linker of nucleoskeleton and cytoskeleton complex protein nesprin-1 at 6 months of age (Fig. 6, *B* and

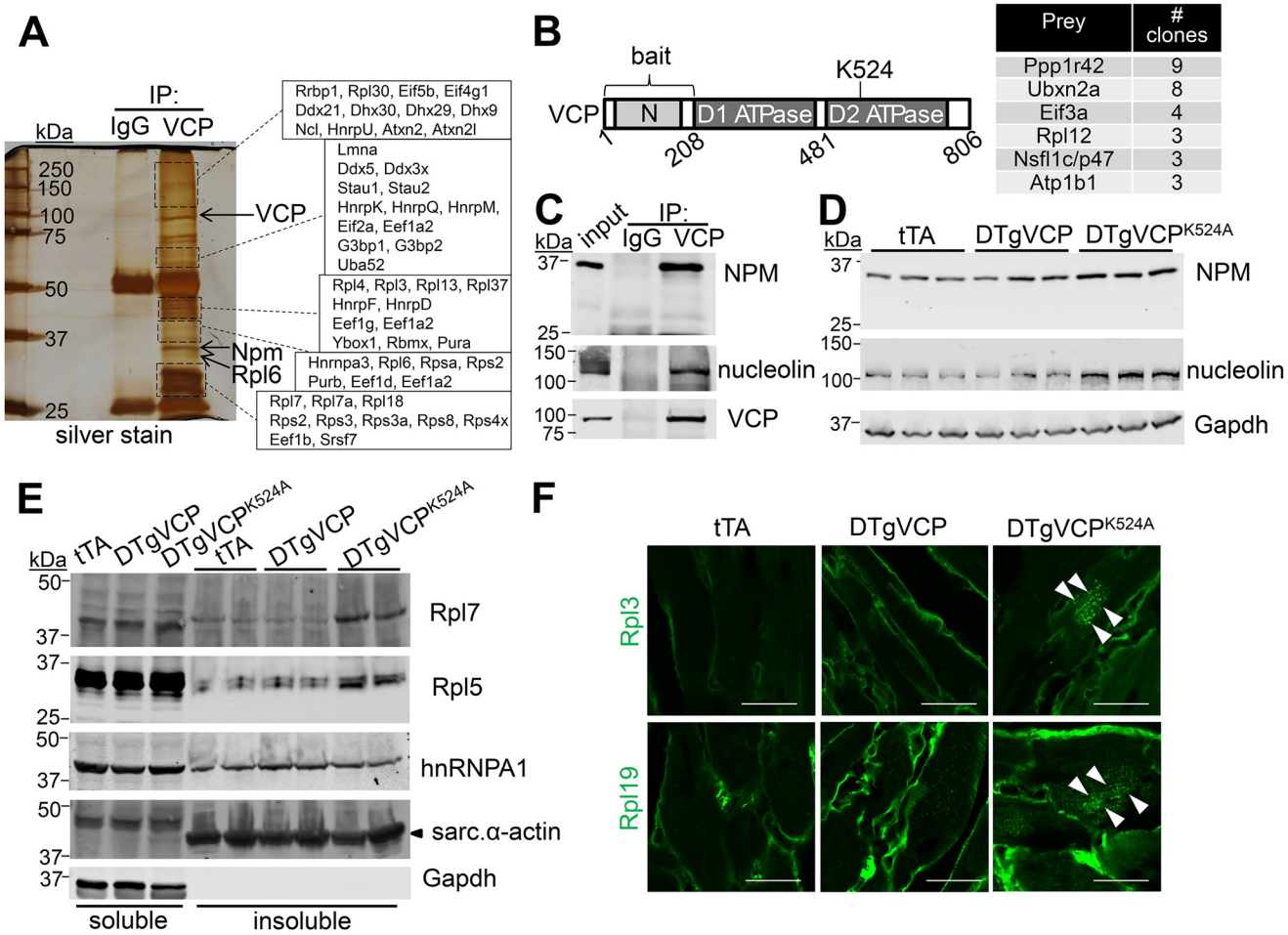

Figure 7. VCP interacts with RBPs, nucleolar proteins, and ribosomal proteins in the heart. *A*, VCP was immunoprecipitated (*IP*) from cardiac lysates from 2-month-old WT mice, and immunoprecipitated proteins were sequenced by MS. RBPs, ribonucleoproteins, and ribosomal proteins were overwhelmingly enriched in the VCP cardiac interactome. The full dataset is available in the supporting information. *B*, schematic of the domain structure of VCP used for yeast two-hybrid screening with the N-terminal cofactor-binding domain of VCP as bait, which also identified ribosomal and translational proteins as direct interactors of VCP. The table lists all prey plasmids sequenced three or more times of 41 unique interacting proteins identified and 66 sequenced prey clones in total. *C*, immunoprecipitation of VCP from mouse heart protein lysates, followed by immunoblotting for NPM and nucleolin. IgG immunoprecipitation was used as a control. *D*, Western blot for NPM and nucleolin in transgenic hearts at 6 months of age from the indicated genotypes of mice. Gapdh was used as a processing and loading control. *E*, Western blot to detect aggregation of the indicated proteins using Triton-soluble and -insoluble protein pellets (later made soluble with urea) of cardiac extracts from the indicated genotypes at 6 months of age. *F*, representative immunohistochemistry for the indicated large ribosomal subunit proteins (*green*) in cardiac cryosections from transgenic mice of the indicated genotypes at 6 months of age. *Scale bar* = 10 μm. *Arrowheads* indicate areas with aggregated Rpl3 or Rpl19 exclusively in DTgVCP^{K524A} hearts.

C). Lamin-associated polypeptide 2β (LAP2β), an INM protein (49, 50), was up-regulated in hearts overexpressing WT VCP or VCP^{K524A} at 2 and 6 months of age (Fig. 6, *B* and *C*), suggesting that VCP forms a complex with LAP2β at the cardiomyocyte inner nuclear membrane. However, the expression of the structurally related INM protein MAN1 was unaltered by VCP overexpression (Fig. 6*B*). Indeed, VCP has been reported to function in a protein quality control pathway at the INM (25, 26), which may also be the case in cardiomyocytes. In conclusion, impairment VCP ATPase activity in the heart is sufficient to cause severe defects in the structure and molecular composition of cardiomyocyte nuclei.

The VCP interactome implies a role in cardiac ribostasis

In an effort to gain further mechanistic insight into the molecular functions of VCP in the heart, we performed proteomics to identify VCP-interacting proteins by immunoprecipitating endogenous VCP from mouse hearts and performing unbiased mass spectroscopy (MS)-based peptide analysis. Notably, we identified a profound enrichment of RBPs, ribosomal proteins and translation factors, nucleolar proteins, and ribonucleoproteins (RNPs) in the cardiac VCP interactome (Fig. 7*A* and Table S1). These include the known VCP interactor and RBP Ataxin-2 (51) and several "L" ribosomal proteins (Rpl proteins) that compose the large ribosomal subunit, ribosomal "S" proteins (Rps proteins) that compose the small ribosomal subunit, ribosome-binding protein 1 (Rrbp1), and Uba52, a fusion protein of ubiquitin with Rpl40 (52). Also identified were eukaryotic elongation factors and translation initiation factors, heterogeneous nuclear ribonucleoproteins (hnRNPs), DEAD-box RNA helicases (Ddx and Dhx proteins), and the nucleolar proteins nucleophosmin (NPM) and nucleolin (Fig. 7*A*). Importantly, many of these VCP-interacting proteins have been identified as components of RNP granules, higher-order cytoplasmic complexes of RNA and RBPs that accumulate in response to translation inhibition. These include

hnRNPs, staufens (Stau1 and Stau2), G3BP1/2, Ddx helicases, and euakaryotic initiation and elongation factors (53–57). Taken together, these data suggest that VCP has important functions in the regulation of ribosome remodeling and assembly and/or dissociation of complexes of ribosomal proteins, RNA, and RBPs, which could affect RNP granule dynamics and ribosome homeostasis.

As a complementary experimental approach to discover proteins that directly associate with VCP, we performed yeast two-hybrid (Y2H) screening using the N-terminal cofactor binding domain of VCP as bait (Fig. 7*B*). The known VCP cofactors Nsfl1c (also known as p47) (17) and Ubxn2a (58) were sequenced several times (Fig. 5*B*), validating the Y2H approach. Importantly, the large ribosomal subunit protein Rpl12 and the translation initiation factor Eif3a were also sequenced several times (Fig. 7*B*), substantiating the association of VCP with ribosomal and ribosome-associated proteins in the heart (Fig. 7*A*). The small ribosomal subunit protein Rps20 and the known VCP cofactor Ufd1 (30) were also among the 41 unique clones identified by Y2H screening (data not shown). Thus, unbiased proteomics approaches collectively indicate predominant interactions of VCP with RBPs, ribosomal proteins, and ribosome-associated proteins.

It is also noteworthy that VCP was found to interact with the nucleolar proteins NPM and nucleolin in the heart (Fig. 7*A*), which was confirmed by immunoprecipitation of VCP and Western blotting (Fig. 7*C*). Moreover, NPM and nucleolin protein levels are up-regulated in VCP^{K524A} hearts (Fig. 7*D*). VCP has been reported previously to function in the nucleolus (59), which serves as the preliminary site of ribosome biogenesis (33). Thus, VCP could potentially participate in processing or maturation of rRNA and preribosomes in cardiomyocyte nucleoli.

To investigate the functional consequence of the association of VCP with ribosomes and ribosome-associated proteins in cardiomyocytes, we processed hearts from transgenic mice into Triton-soluble and insoluble fractions and performed immunoblotting for ribosomal proteins. There was a substantial increase in the large ribosomal subunit proteins Rpl5 and Rpl7 in the insoluble fraction in hearts overexpressing ATPase-deficient VCP (Fig. 7*E*), suggesting that ribosomal proteins aggregate when cardiomyocyte VCP activity is inhibited. Immunohistochemistry further revealed accumulation and aggregation of the large ribosomal subunit proteins Rpl3 and Rpl19 in $DTgVCP^{K524A}$ cardiomyocytes (Fig. 7*F*), suggesting important cardiac functions for VCP in ribosome assembly, turnover, and/or remodeling. However, acute pharmacological inhibition of VCP activity in rat neonatal cardiomyocytes did not disrupt large ribosomal subunit protein localization (Fig. S4), suggesting that aggregation of ribosomal proteins caused by genetic inhibition of VCP activity in the heart may be secondary to abnormal ERAD activity and dysregulation of proteostasis. Indeed, genetic deletion of the ERAD component Sel1L in mouse pancreas also results in aggregation of ribosomal proteins (37), indicating that ERAD may functionally couple protein degradation and ER protein quality control with translation machinery to orchestrate synchronized regulation of proteostasis *in vivo*.

Discussion

Cardiomyocyte VCP activity is required for cardiac homeostasis and ERAD

Mutations in *VCP* cause multisystem proteinopathy 1 or IBMPFD, which affect skeletal muscle, brain, bone, and heart and account for roughly 50% of all familial multisystem proteinopathy disorders (60). Mutations in *VCP* are also thought to be responsible for 1–2% of familial ALS (61). The vast majority of the disease-causing mutations are missense mutations in the N-terminal cofactor and ubiquitin binding domain of VCP distal from its ATPase domains (62, 63); however, the underlying molecular etiology of these mutations and the mechanisms by which they cause disease are unclear. Therefore, to directly interrogate the functions of VCP in the heart, we mutated the Lys-524 residue within the D2 ATPase domain of VCP, which is known to be required for its activity (8).

Disruption of cardiomyocyte VCP ATPase activity *in vivo* by overexpression of an ATPase-deficient VCP^{K524A} mutant resulted in age-dependent cardiomyopathy and an exacerbated cardiac disease response to pressure overload, underscoring the crucial functions of VCP in cardiac physiology and adaptive responsiveness. VCP is known to function in a myriad of ubiquitin-dependent cellular protein quality control pathways, including its well-described translocase functions in the ERAD pathway, where VCP extracts misfolded proteins from the ER for degradation by the UPS (7, 11–14, 16). Hearts overexpressing the VCP^{K524A} mutant accumulated ubiquitinated proteins and up-regulated several ER membrane and ER luminal proteins that participate in the ERAD pathway, which is likely a compensatory response because of defective clearance of ERAD substrates in these cardiomyocytes. Interestingly, transgenic hearts overexpressing either WT or mutant VCP up-regulated protein expression of the ER membrane adaptor Sel1L, suggesting a stoichiometric complex between these two proteins. Expression of Sel1L is a critical determinant of the stability of the ERAD complex, including regulation of the requisite ERAD E3 ligase Hrd1 in the ER membrane (38). Thus, hearts overexpressing WT VCP likely enhance the stability and expression of a functional ERAD complex, whereas VCP^{K524A} overexpressing hearts up-regulate the ERAD pathway, likely in a nonfunctional manner whereby misfolded substrates in the ER are fed into the ERAD complex and ubiquitinated but unable to be dislocated for degradation by the UPS. Indeed, similar to what we observed with inhibition of cardiac VCP activity, genetic knockdown of Hrd1 results in cardiac hypertrophy at baseline and augmented cardiomyopathy in response to pressure overload (36), providing further evidence of the critical role of ERAD in cardiac homeostasis and the response of the heart to pathological stress.

A previous study found a reduction in cardiac hypertrophy 2 weeks after TAC-induced pressure overload in cardiomyocyte-specific transgenic mice overexpressing WT VCP (64). Although we did not evaluate cardiac structure in our transgenic VCP mouse models until 4 and 8 weeks after TAC surgery, no reduction in cardiac hypertrophy was observed. Our WT VCP transgenic mice were generated on the same genetic background (FVB/N), and expression was also driven by the

α-MHC promoter, achieving similar robust overexpression as the previously reported transgenic model (64). Based on our results, it is likely that VCP overexpression in the heart only has minimal functional effects, given its already high abundance, accounting for upward of 1% of total cellular protein (65–67).

VCP activity is necessary to maintain cardiomyocyte nuclear integrity

Expression of the VCP^{K524A} mutant in the mouse heart caused a dramatic alteration in nuclear morphology along with the appearance of intranuclear vesicles for the first time, as well as alterations in the molecular composition of the nuclear envelope and nuclear lamina. Although VCP has been reported to be involved in assembly of the nuclear envelope (23), we did not observe defects in cardiomyocyte nuclear morphology in $DTgVCP^{K524A}$ hearts until 5 months of age, suggesting that VCP does not directly mediate envelope assembly.

Interestingly, there was a stoichiometric up-regulation of the lamin-binding INM protein LAP2β with overexpression of either WT or mutant VCP at 2 months of age, suggesting that VCP forms a complex with LAP2β at the cardiomyocyte INM. Indeed, we observed VCP both in the cytoplasm and the nucleus in cardiomyocytes, as reported in other cell types (25, 26, 59, 68). The VCP homolog Cdc48 also functions in an INM quality control pathway of yeast (25, 26), and because the nuclear envelope is contiguous with the ER, it is possible that VCP functions in a pathway at the cardiomyocyte INM analogous to ERAD in the ER to regulate proteostasis of this entire linked compartment. Intranuclear aggregates are observed in cardiac and skeletal muscle myocytes from patients with IBMPFD (3, 69), suggesting that the nuclear protein quality control functions of VCP may contribute to the molecular etiology of human disease. Indeed, the heart is particularly susceptible to disease caused by mutations in genes encoding proteins of the nuclear lamina or nuclear envelope (49, 70). Thus, cardiomyocyte nuclear defects likely contribute to cardiomyopathy in VCP^{K524A} mice.

VCP activity and cardiac ribostasis

VCP can also function in ribosome-associated quality control to facilitate the release of polypeptides stalled in translation on ribosomes for degradation by the proteasome (27, 28, 30). We found that VCP directly interacts with ribosomal proteins, and impairment of cardiac VCP ATPase activity causes ribosomal protein aggregation, suggesting that VCP functions in ribosome biogenesis and/or remodeling in cardiomyocytes. VCP could participate in ribosome biogenesis within the cardiomyocyte nucleolus, particularly given its interaction with NPM and nucleolin, which could directly affect ribosome assembly and formation. Indeed, EM imaging of VCP^{K524A} hearts at 10 months of age showed electron-opaque regions emanating from what appeared to be the nucleolus, as if these were regions with accumulating condensed ribonuclear proteins (Fig. 6*A*). Indeed, we also observed aggregation of large ribosomal subunit proteins in the cardiomyocyte cytoplasm when VCP activity was inhibited, suggesting that VCP can function in ribosome processing, shuttling, turnover, or remodeling in the nucleus and cytoplasm. Unbiased proteomics identified associations of VCP with ribosomal proteins and translation factors, supporting a role of VCP in cardiomyocyte ribostasis.

It is possible that VCP^{K524A} hearts exhibit aberrant ribosome quality control as a secondary response to stalled translation downstream of activation of the UPR. However, we observed specific and prominent effects on the ERAD pathway in VCP^{K524A} hearts and believe that induction of PERK and activation ATF6α occur as a secondary response to enhance the protein folding capacity of the ER to compensate for defective ER protein quality control. ER stress alone could not account for the direct interaction of VCP with ribosomes nor its previously established functions in translation stress (27), suggesting that VCP could have direct effects on ribostasis in the heart. Our data indicate that VCP inhibition causes primary defects in ribosome quality control that take time to manifest in the adult heart to ultimately contribute to or even induce cardiomyopathy, as reminiscent of multisystem proteinopathy in the heart and other tissues caused by *VCP* mutations in human patients.

Overall, our results identify that VCP activity is critical for cardiac homeostasis and function. We found that VCP activity is necessary for proper cardiac ERAD and ribostasis as well as maintenance of cardiomyocyte nuclear structure. These pleiotropic phenotypes resulting from impaired VCP activity underscore the multifaceted molecular mechanisms whereby *VCP* mutations may cause disease in multiple organ systems in humans, especially in the heart.

Experimental procedures

Animals

Transgenic mice with cardiomyocyte-specific overexpression of WT VCP or VCP containing a point mutation of lysine 524 to alanine (K524A) were generated using the bigenic α-MHC promoter-driven transgene system (35), as described previously (71, 72). All mice were generated on the FVB/N genetic background. Briefly, a mouse VCP cDNA (Dharmacon, MMM1013-202859349) was subcloned into the SalI and HindIII restriction sites of the α-MHC promoter expression vector (35), and the resulting construct was digested with NotI to gel-purify the promoter–cDNA fragment for oocyte injection by the Transgenic Animal and Genome Editing Research Core at Cincinnati Children's Hospital. To generate the VCP^{K524A} mutant construct, mutagenesis was performed using the QuikChange II XL site-directed mutagenesis kit (Agilent Technologies) and the following primers: forward, 5′-GACCTCCTGGCTGTGGGGCAACCTTACTGGCTAAAG-3′; reverse, 5′-CTTTAGCCAGTAGGTTGCCCCACAGCCAGGAGGTC-3′.

Transgenic mice in the FVB/N genetic background were bred and maintained on normal lab chow in the absence of tetracycline or doxycycline so that the bigenic α-MHC promoter-driven system remains fully induced at all times, which begins around birth in ventricular cardiomyocytes (35). Because no disease was observed in VCP transgenic mice, and disease in VCP^{K524A} mice was not observed until after 6 months, we did not need to use the inducibility of this bigenic system. Echocardiography to evaluate cardiac function (72) and TAC to surgically induce pressure overload hypertrophy in 8-

to 10-week-old mice (73) were performed as described previously. All animal procedures were approved by the Cincinnati Children's Institutional Animal Care and Use Committee (protocol 2016-0069) and conformed to the NIH Guide for the Care and Use of Laboratory Animals. The number of mice used in this study reflects the minimum number of mice needed to achieve statistical significance (see "Statistical analysis"). The animals were not randomized and handled in a blinded manner, and both sexes were used. Analgesics were given to mice after the TAC surgical procedure to reduce pain (buprenorphine given subcutaneously at 0.1 mg/kg).

Cultured neonatal rat cardiomyocytes

Primary rat neonatal cardiomyocytes were cultured from dissociated hearts of 1- to 2-day-old neonatal rats exactly as described previously (72). Cardiomyocytes were cultured in M199 medium (Corning) with 1% BGS (Hyclone) for 48 h and then treated with DeBQ (Sigma-Aldrich) in M199 medium with 1% bovine growth serum for 8 h prior to harvesting for Western blotting.

Western blotting

Western blotting was performed as described previously (71). Proteins were extracted from mouse hearts or cultured cardiomyocytes in radioimmune precipitation assay buffer (50 mM Tris·HCl (pH 7.4), 1% Triton X-100, 1% sodium deoxycholate, 1 mM EDTA, and 0.1% SDS) with Halt protease inhibitors (Thermo Fisher Scientific) and sonicated with a Bioruptor UCD-200 (Diagenode), and lysates were cleared by centrifugation at 14,000 rpm for 10 min at 4 °C. Fractionation of mouse hearts into soluble and insoluble fractions was performed as described previously (74) with modifications. Hearts were homogenized in NET buffer (20 mM Tris·HCl (pH 8.0), 100 mM NaCl, and 1 mM EDTA) with 1% Triton X-100 and protease inhibitors, sonicated, and clarified by centrifugation at 20,000 × *g* for 20 min at 4 °C, and then the supernatant was saved as the Triton-soluble fraction. The pellet was washed twice with PBS and protease inhibitors and then resuspended in urea buffer (7 M urea, 2 M thiourea, 4% CHAPS, and 30 mM Tris (pH 8.5)) with protease inhibitors, passed through an 21-gauge needle 10 times, sonicated, and clarified by centrifugation at 20,000 × *g* for 10 min at 4 °C to generate the insoluble fraction. Protein concentrations were determined using the DC Protein Assay (Bio-Rad) or the Pierce 660 nm Protein Assay (Thermo Fisher Scientific). Lysates were boiled in Laemmli buffer, resolved by SDS-PAGE, and transferred to PVDF membranes (Immobilon-FL, Millipore) for immunoblotting. Primary antibodies used were VCP (Abcam, ab36047, 1:500 or Novus Biologicals, NBP120-11433, 1:1,000), Gapdh (Fitzgerald, 10R-G109A, 1:50,000), ubiquitin (Enzo, BML-PW0930-0100, 1:500), Sel1L (Abcam, ab78298, 1:1,000), OS-9 (Abcam, ab109510, 1:500), Herp (Abcam, ab73669, 1:500), cyclophilin B (Abcam, ab16045, 1:2,000), calnexin (Cell Signaling Technology, 2433, 1:500), protein disulfide isomerase (Cell Signaling Technology, 2446S, 1:500), BiP (Sigma, G8918, 1:2000), α-tubulin (Sigma, T5168, 1:1,000), ATF6α-N (Signalway, SAB24383, 1:1,000), PERK (Cell Signaling Technology, 3192S, 1:1,000), IRE1α (Cell Signaling Technology, 3294S, 1:1,000), p-IRE1α (Abcam, ab48187, 1:1,000), Xbp1-s (Cell Signaling Technology, 83418S, 1:1,000), lamin A/C (Cell Signaling Technology, 2032, 1:500), lamin B1 (Cell Signaling Technology, 12586, 1:1,000), LAP2β (Bethyl Laboratories, A304-840A, 1:500), nesprin-1 (Abcam, ab192234, 1:500), nesprin-2 (Novus Biologicals, NBP1-84190, 1:500), SUN2 (Abcam, ab124916, 1:500), MAN1 (Santa Cruz Biotechnology, sc-50458, 1:500), Ran (Abcam, ab157213, 1:500), Gata4 (Santa Cruz Biotechnology, sc-1237, 1:250), Rpl7 (Abcam, ab72550, 1:500), Rpl5 (Abcam, ab86863, 1:500), hnRNPA1 (Abcam, ab50492, 1:500), α-sarcomeric actin (Sigma, A2172, 1:15,000), nucleophosmin (Abcam, ab10530, 1:500), and nucleolin (Abcam, ab22758, 1:1,000). Primary antibodies were followed by the appropriate fluorescent secondary antibodies (LI-COR Biosciences) and detection on an Odyssey CLx scanner (LI-COR Biosciences).

Transmission EM and immunohistochemistry

EM was performed on mouse cardiac tissue exactly as described previously (72). Hearts were perfusion-fixed in glutaraldehyde/cacodylate buffer, embedded in epoxy resin for sectioning, and then counterstained and imaged on a transmission electron microscope. Immunohistochemistry (IHC) was performed as described elsewhere (73, 75). Hearts were fixed in 4% paraformaldehyde for 4 h, incubated in 30% sucrose overnight, embedded in O.C.T (Tissue-Tek), frozen, and cryosectioned. Cryosections were fixed in methanol at −20 °C for 10 min, washed in PBS, blocked in IHC buffer (PBS, 5% goat serum, 1% BSA, 1% glycine, and 0.2% Triton X-100) for 1 h at room temperature, and then incubated with anti-Rpl3 (Proteintech, 66130-1-Ig) or anti-Rpl19 (Abnova, H00006143-M01) antibodies diluted 1:50 in IHC buffer overnight at 4 °C. Sections were then incubated with Alexa Fluor secondary antibodies (Thermo Fisher Scientific) diluted 1:1000 in IHC buffer for 1 h at room temperature and mounted with ProLong Gold Antifade Mountant (Thermo Fisher Scientific). Cultured neonatal rat cardiomyocytes were fixed in 4% paraformaldehyde and stained similarly using anti-Rpl6 (GeneTex, GTX114913, 1:50) or anti-Rpl7 (Abcam, ab72550, 1:100) antibodies. Staining with wheat germ agglutinin (Invitrogen) and quantification of cell surface area was performed in paraffin-embedded cardiac sections as described previously (72, 76). Image acquisition was performed on a Nikon A1 confocal microscope.

Immunoprecipitation, Y2H, and proteomics

Immunoprecipitation of mouse cardiac lysates was performed as described elsewhere (71). Mouse hearts were homogenized in lysis buffer (25 mM Tris·HCl (pH 7.4) and 5 mM EDTA) with protease inhibitors using a Dounce homogenizer. The lysate was spun down at 3,000 × *g* for 5 min at 4 °C, and the pellet was resuspended in NET buffer with 1% Triton X-100 and protease inhibitors, sonicated, and then immunoprecipitated with 5 μg of anti-VCP antibody (Novus Biologicals, NBP120-11433) or IgG control (Santa Cruz Biotechnology) coupled to protein G Dynabeads (Thermo Fisher Scientific). Immunoprecipitates were washed three times in NET buffer with 1% Triton X-100 and boiled in Laemmli buffer for SDS-PAGE. Protein gels were transferred to PVDF membranes for Western blotting as described above or stained with the Prote-

oSilver Silver Stain Kit (Sigma) and submitted to the University of Cincinnati Proteomics Core Laboratory for MS sequencing by nano-LC-MS/MS and MALDI-TOF.

Yeast two-hybrid screening was performed as described previously (76) using the N-terminal domain (amino acids 1 to 208) of mouse VCP as bait and a mouse embryo cDNA prey library (Clontech). Plasmids purified from growing colonies were sequenced at the Cincinnati Children's Hospital DNA Sequencing Core, and the identities of prey plasmids were determined using the Basic Local Alignment Search Tool (NCBI).

Quantitative real-time PCR (qPCR)

qPCR was performed exactly as described previously (76). Briefly, RNA was isolated from mouse cardiac tissue using the RNEasy fibrous tissue mini kit (Qiagen). cDNA was synthesized using the Verso cDNA synthesis Kit (Thermo Scientific), and qPCR was performed with gene-specific primers and SsoAdvanced Universal SYBR Green Supermix (Bio-Rad) on a CFX96 Real-Time PCR Detection System (Bio-Rad). The primer sequences for *Sel1L* (77), *OS9* (37), and *Herpud1* (78) are published elsewhere. The primer sequences for *Gapdh* were as follows: forward, 5′-TGCCCCCATGTTTGTGATG-3′; reverse, 5′-TGTGGTCATGAGCCCTTCC-3′. Expression was quantified using the standard curve method and normalized to Gapdh expression.

Statistical analysis

Data are represented as the mean ± S.D., and testing for statistical significance was performed using one-tailed Student's *t* test or one-way analysis of variance (ANOVA) with post hoc Tukey's test.

Author contributions—M. J. B. and J. D. M. conceptualization; M. J. B., D. V., and C. V. B. data curation; M. J. B. and J. D. M. formal analysis; M. J. B., R. L., R. N. C., and M. A. S. investigation; J. D. M. resources; J. D. M. supervision; J. D. M. funding acquisition; J. D. M. project administration; J. D. M. writing - review and editing.

References

1. Custer, S. K., Neumann, M., Lu, H., Wright, A. C., and Taylor, J. P. (2010) Transgenic mice expressing mutant forms VCP/p97 recapitulate the full spectrum of IBMPFD including degeneration in muscle, brain and bone. *Hum. Mol. Genet.* **19,** 1741–1755 CrossRef Medline
2. Badadani, M., Nalbandian, A., Watts, G. D., Vesa, J., Kitazawa, M., Su, H., Tanaja, J., Dec, E., Wallace, D. C., Mukherjee, J., Caiozzo, V., Warman, M., and Kimonis, V. E. (2010) VCP associated inclusion body myopathy and Paget disease of bone knock-in mouse model exhibits tissue pathology typical of human disease. *PLoS ONE* **5,** e13183 CrossRef Medline
3. Hübbers, C. U., Clemen, C. S., Kesper, K., Böddrich, A., Hofmann, A., Kämäräinen, O., Tolksdorf, K., Stumpf, M., Reichelt, J., Roth, U., Krause, S., Watts, G., Kimonis, V., Wattjes, M. P., Reimann, J., *et al.* (2007) Pathological consequences of VCP mutations on human striated muscle. *Brain* **130,** 381–393 CrossRef Medline
4. Watts, G. D., Wymer, J., Kovach, M. J., Mehta, S. G., Mumm, S., Darvish, D., Pestronk, A., Whyte, M. P., and Kimonis, V. E. (2004) Inclusion body myopathy associated with Paget disease of bone and frontotemporal dementia is caused by mutant valosin-containing protein. *Nat. Genet.* **36,** 377–381 CrossRef Medline
5. Meyer, H., Bug, M., and Bremer, S. (2012) Emerging functions of the VCP/p97 AAA-ATPase in the ubiquitin system. *Nat. Cell Biol.* **14,** 117–123 CrossRef Medline
6. Kloppsteck, P., Ewens, C. A., Förster, A., Zhang, X., and Freemont, P. S. (2012) Regulation of p97 in the ubiquitin-proteasome system by the UBX protein family. *Biochim. Biophys. Acta* **1823,** 125–129 CrossRef Medline
7. DeLaBarre, B., Christianson, J. C., Kopito, R. R., and Brunger, A. T. (2006) Central pore residues mediate the p97/VCP activity required for ERAD. *Mol. Cell* **22,** 451–462 CrossRef Medline
8. Kobayashi, T., Tanaka, K., Inoue, K., and Kakizuka, A. (2002) Functional ATPase activity of p97/valosin-containing protein (VCP) is required for the quality control of endoplasmic reticulum in neuronally differentiated mammalian PC12 cells. *J. Biol. Chem.* **277,** 47358–47365 CrossRef Medline
9. DeLaBarre, B., and Brunger, A. T. (2003) Complete structure of p97/valosin-containing protein reveals communication between nucleotide domains. *Nat. Struct. Biol.* **10,** 856–863 CrossRef Medline
10. Alexandru, G., Graumann, J., Smith, G. T., Kolawa, N. J., Fang, R., and Deshaies, R. J. (2008) UBXD7 binds multiple ubiquitin ligases and implicates p97 in HIF1α turnover. *Cell* **134,** 804–816 CrossRef Medline
11. Rabinovich, E., Kerem, A., Fröhlich, K. U., Diamant, N., and Bar-Nun, S. (2002) AAA-ATPase p97/Cdc48p, a cytosolic chaperone required for endoplasmic reticulum-associated protein degradation. *Mol. Cell Biol.* **22,** 626–634 CrossRef Medline
12. Ye, Y., Meyer, H. H., and Rapoport, T. A. (2001) The AAA ATPase Cdc48/p97 and its partners transport proteins from the ER into the cytosol. *Nature* **414,** 652–656 CrossRef Medline
13. Ye, Y., Shibata, Y., Kikkert, M., van Voorden, S., Wiertz, E., and Rapoport, T. A. (2005) Recruitment of the p97 ATPase and ubiquitin ligases to the site of retrotranslocation at the endoplasmic reticulum membrane. *Proc. Natl. Acad. Sci. U.S.A.* **102,** 14132–14138 CrossRef Medline
14. Greenblatt, E. J., Olzmann, J. A., and Kopito, R. R. (2011) Derlin-1 is a rhomboid pseudoprotease required for the dislocation of mutant α-1 antitrypsin from the endoplasmic reticulum. *Nat. Struct. Mol. Biol.* **18,** 1147–1152 CrossRef Medline
15. Heo, J. M., Livnat-Levanon, N., Taylor, E. B., Jones, K. T., Dephoure, N., Ring, J., Xie, J., Brodsky, J. L., Madeo, F., Gygi, S. P., Ashrafi, K., Glickman, M. H., and Rutter, J. (2010) A stress-responsive system for mitochondrial protein degradation. *Mol. Cell* **40,** 465–480 CrossRef Medline
16. Ye, Y., Meyer, H. H., and Rapoport, T. A. (2003) Function of the p97-Ufd1-Npl4 complex in retrotranslocation from the ER to the cytosol: dual recognition of nonubiquitinated polypeptide segments and polyubiquitin chains. *J. Cell Biol.* **162,** 71–84 CrossRef Medline
17. Kondo, H., Rabouille, C., Newman, R., Levine, T. P., Pappin, D., Freemont, P., and Warren, G. (1997) p47 is a cofactor for p97-mediated membrane fusion. *Nature* **388,** 75–78 CrossRef Medline
18. Ramadan, K., Bruderer, R., Spiga, F. M., Popp, O., Baur, T., Gotta, M., and Meyer, H. H. (2007) Cdc48/p97 promotes reformation of the nucleus by extracting the kinase Aurora B from chromatin. *Nature* **450,** 1258–1262 CrossRef Medline
19. Maric, M., Maculins, T., De Piccoli, G., and Labib, K. (2014) Cdc48 and a ubiquitin ligase drive disassembly of the CMG helicase at the end of DNA replication. *Science* **346,** 1253596 CrossRef Medline
20. Moreno, S. P., Bailey, R., Campion, N., Herron, S., and Gambus, A. (2014) Polyubiquitylation drives replisome disassembly at the termination of DNA replication. *Science* **346,** 477–481 CrossRef Medline
21. Meerang, M., Ritz, D., Paliwal, S., Garajova, Z., Bosshard, M., Mailand, N., Janscak, P., Hübscher, U., Meyer, H., and Ramadan, K. (2011) The ubiquitin-selective segregase VCP/p97 orchestrates the response to DNA double-strand breaks. *Nat. Cell Biol.* **13,** 1376–1382 CrossRef Medline
22. Shih, Y. T., and Hsueh, Y. P. (2016) VCP and ATL1 regulate endoplasmic reticulum and protein synthesis for dendritic spine formation. *Nat. Commun.* **7,** 11020 CrossRef Medline
23. Hetzer, M., Meyer, H. H., Walther, T. C., Bilbao-Cortes, D., Warren, G., and Mattaj, I. W. (2001) Distinct AAA-ATPase p97 complexes function in discrete steps of nuclear assembly. *Nat. Cell Biol.* **3,** 1086–1091 CrossRef Medline

24. Zhou, H. L., Geng, C., Luo, G., and Lou, H. (2013) The p97-UBXD8 complex destabilizes mRNA by promoting release of ubiquitinated HuR from mRNP. *Genes Dev.* **27,** 1046–1058 CrossRef Medline
25. Foresti, O., Rodriguez-Vaello, V., Funaya, C., and Carvalho, P. (2014) Quality control of inner nuclear membrane proteins by the Asi complex. *Science* **346,** 751–755 CrossRef Medline
26. Pantazopoulou, M., Boban, M., Foisner, R., and Ljungdahl, P. O. (2016) Cdc48 and Ubx1 participate in a pathway associated with the inner nuclear membrane that governs Asi1 degradation. *J. Cell Sci.* **129,** 3770–3780 CrossRef Medline
27. Brandman, O., Stewart-Ornstein, J., Wong, D., Larson, A., Williams, C. C., Li, G. W., Zhou, S., King, D., Shen, P. S., Weibezahn, J., Dunn, J. G., Rouskin, S., Inada, T., Frost, A., and Weissman, J. S. (2012) A ribosome-bound quality control complex triggers degradation of nascent peptides and signals translation stress. *Cell* **151,** 1042–1054 CrossRef Medline
28. Defenouillère, Q., Yao, Y., Mouaikel, J., Namane, A., Galopier, A., Decourty, L., Doyen, A., Malabat, C., Saveanu, C., Jacquier, A., and Fromont-Racine, M. (2013) Cdc48-associated complex bound to 60S particles is required for the clearance of aberrant translation products. *Proc. Natl. Acad. Sci. U.S.A.* **110,** 5046–5051 CrossRef Medline
29. Defenouillère, Q., Zhang, E., Namane, A., Mouaikel, J., Jacquier, A., and Fromont-Racine, M. (2016) Rqc1 and Ltn1 prevent C-terminal alanine-threonine tail (CAT-tail)-induced protein aggregation by efficient recruitment of Cdc48 on stalled 60S subunits. *J. Biol. Chem.* **291,** 12245–12253 CrossRef Medline
30. Verma, R., Oania, R. S., Kolawa, N. J., and Deshaies, R. J. (2013) Cdc48/p97 promotes degradation of aberrant nascent polypeptides bound to the ribosome. *Elife* **2,** e00308 Medline
31. An, H., and Harper, J. W. (2018) Systematic analysis of ribophagy in human cells reveals bystander flux during selective autophagy. *Nat. Cell Biol.* **20,** 135–143 CrossRef Medline
32. Deisenroth, C., and Zhang, Y. (2010) Ribosome biogenesis surveillance: probing the ribosomal protein-Mdm2-p53 pathway. *Oncogene.* **29,** 4253–4260 CrossRef Medline
33. Thomson, E., Ferreira-Cerca, S., and Hurt, E. (2013) Eukaryotic ribosome biogenesis at a glance. *J. Cell Sci.* **126,** 4815–4821 CrossRef Medline
34. Lynch, J. M., Maillet, M., Vanhoutte, D., Schloemer, A., Sargent, M. A., Blair, N. S., Lynch, K. A., Okada, T., Aronow, B. J., Osinska, H., Prywes, R., Lorenz, J. N., Mori, K., Lawler, J., Robbins, J., and Molkentin, J. D. (2012) A thrombospondin-dependent pathway for a protective ER stress response. *Cell* **149,** 1257–1268 CrossRef Medline
35. Sanbe, A., Gulick, J., Hanks, M. C., Liang, Q., Osinska, H., and Robbins, J. (2003) Reengineering inducible cardiac-specific transgenesis with an attenuated myosin heavy chain promoter. *Circ. Res.* **92,** 609–616 CrossRef Medline
36. Doroudgar, S., Völkers, M., Thuerauf, D. J., Khan, M., Mohsin, S., Respress, J. L., Wang, W., Gude, N., Müller, O. J., Wehrens, X. H., Sussman, M. A., and Glembotski, C. C. (2015) Hrd1 and ER-associated protein degradation, ERAD, are critical elements of the adaptive ER stress response in cardiac myocytes. *Circ. Res.* **117,** 536–546 CrossRef Medline
37. Sun, S., Shi, G., Han, X., Francisco, A. B., Ji, Y., Mendonça, N., Liu, X., Locasale, J. W., Simpson, K. W., Duhamel, G. E., Kersten, S., Yates, J. R., 3rd, Long, Q., and Qi, L. (2014) Sel1L is indispensable for mammalian endoplasmic reticulum-associated degradation, endoplasmic reticulum homeostasis, and survival. *Proc. Natl. Acad. Sci. U.S.A.* **111,** E582–E591 CrossRef Medline
38. Iida, Y., Fujimori, T., Okawa, K., Nagata, K., Wada, I., and Hosokawa, N. (2011) SEL1L protein critically determines the stability of the HRD1-SEL1L endoplasmic reticulum-associated degradation (ERAD) complex to optimize the degradation kinetics of ERAD substrates. *J. Biol. Chem.* **286,** 16929–16939 CrossRef Medline
39. Jeong, H., Sim, H. J., Song, E. K., Lee, H., Ha, S. C., Jun, Y., Park, T. J., and Lee, C. (2016) Crystal structure of SEL1L: Insight into the roles of SLR motifs in ERAD pathway. *Sci. Rep.* **6,** 20261 CrossRef Medline
40. Mueller, B., Lilley, B. N., and Ploegh, H. L. (2006) SEL1L, the homologue of yeast Hrd3p, is involved in protein dislocation from the mammalian ER. *J. Cell Biol.* **175,** 261–270 CrossRef Medline
41. Leitman, J., Shenkman, M., Gofman, Y., Shtern, N. O., Ben-Tal, N., Hendershot, L. M., and Lederkremer, G. Z. (2014) Herp coordinates compartmentalization and recruitment of HRD1 and misfolded proteins for ERAD. *Mol. Biol. Cell* **25,** 1050–1060 CrossRef Medline
42. Hosokawa, N., Kamiya, Y., Kamiya, D., Kato, K., and Nagata, K. (2009) Human OS-9, a lectin required for glycoprotein endoplasmic reticulum-associated degradation, recognizes mannose-trimmed *N*-glycans. *J. Biol. Chem.* **284,** 17061–17068 CrossRef Medline
43. Price, E. R., Zydowsky, L. D., Jin, M. J., Baker, C. H., McKeon, F. D., and Walsh, C. T. (1991) Human cyclophilin B: a second cyclophilin gene encodes a peptidyl-prolyl isomerase with a signal sequence. *Proc. Natl. Acad. Sci. U.S.A.* **88,** 1903–1907 CrossRef Medline
44. Bernasconi, R., Soldà, T., Galli, C., Pertel, T., Luban, J., and Molinari, M. (2010) Cyclosporine A-sensitive, cyclophilin B-dependent endoplasmic reticulum-associated degradation. *PLoS ONE* **5,** e13008 CrossRef Medline
45. Grubb, S., Guo, L., Fisher, E. A., and Brodsky, J. L. (2012) Protein disulfide isomerases contribute differentially to the endoplasmic reticulum-associated degradation of apolipoprotein B and other substrates. *Mol. Biol. Cell* **23,** 520–532 CrossRef Medline
46. Sakoh-Nakatogawa, M., Nishikawa, S., and Endo, T. (2009) Roles of protein-disulfide isomerase-mediated disulfide bond formation of yeast Mnl1p in endoplasmic reticulum-associated degradation. *J. Biol. Chem.* **284,** 11815–11825 CrossRef Medline
47. Braakman, I., and Hebert, D. N. (2013) Protein folding in the endoplasmic reticulum. *Cold Spring Harb. Perspect. Biol.* **5,** a013201 Medline
48. Bertolotti, A., Zhang, Y., Hendershot, L. M., Harding, H. P., and Ron, D. (2000) Dynamic interaction of BiP and ER stress transducers in the unfolded-protein response. *Nat. Cell Biol.* **2,** 326–332 CrossRef Medline
49. Stroud, M. J., Banerjee, I., Veevers, J., and Chen, J. (2014) Linker of nucleoskeleton and cytoskeleton complex proteins in cardiac structure, function, and disease. *Circ. Res.* **114,** 538–548 CrossRef Medline
50. Chu, A., Rassadi, R., and Stochaj, U. (1998) Velcro in the nuclear envelope: LBR and LAPs. *FEBS Lett.* **441,** 165–169 CrossRef Medline
51. Albrecht, M., Golatta, M., Wüllner, U., and Lengauer, T. (2004) Structural and functional analysis of ataxin-2 and ataxin-3. *Eur. J. Biochem.* **271,** 3155–3170 CrossRef Medline
52. Kobayashi, M., Oshima, S., Maeyashiki, C., Nibe, Y., Otsubo, K., Matsuzawa, Y., Nemoto, Y., Nagaishi, T., Okamoto, R., Tsuchiya, K., Nakamura, T., and Watanabe, M. (2016) The ubiquitin hybrid gene UBA52 regulates ubiquitination of ribosome and sustains embryonic development. *Sci. Rep.* **6,** 36780 CrossRef Medline
53. Jain, S., Wheeler, J. R., Walters, R. W., Agrawal, A., Barsic, A., and Parker, R. (2016) ATPase-modulated stress granules contain a diverse proteome and substructure. *Cell* **164,** 487–498 CrossRef Medline
54. Protter, D. S. W., and Parker, R. (2016) Principles and properties of stress granules. *Trends Cell Biol.* **26,** 668–679 CrossRef Medline
55. Buchan, J. R., Kolaitis, R. M., Taylor, J. P., and Parker, R. (2013) Eukaryotic stress granules are cleared by autophagy and Cdc48/VCP function. *Cell* **153,** 1461–1474 CrossRef Medline
56. Kedersha, N., Panas, M. D., Achorn, C. A., Lyons, S., Tisdale, S., Hickman, T., Thomas, M., Lieberman, J., McInerney, G. M., Ivanov, P., and Anderson, P. (2016) G3BP-Caprin1-USP10 complexes mediate stress granule condensation and associate with 40S subunits. *J. Cell Biol.* **212,** 845–860 CrossRef Medline
57. Aulas, A., Caron, G., Gkogkas, C. G., Mohamed, N. V., Destroismaisons, L., Sonenberg, N., Leclerc, N., Parker, J. A., and Vande Velde, C. (2015) G3BP1 promotes stress-induced RNA granule interactions to preserve polyadenylated mRNA. *J. Cell Biol.* **209,** 73–84 CrossRef Medline
58. Raman, M., Sergeev, M., Garnaas, M., Lydeard, J. R., Huttlin, E. L., Goessling, W., Shah, J. V., and Harper, J. W. (2015) Systematic proteomics of the VCP-UBXD adaptor network identifies a role for UBXN10 in regulating ciliogenesis. *Nat. Cell Biol.* **17,** 1356–1369 CrossRef Medline
59. Partridge, J. J., Lopreiato, J. O., Jr, Latterich, M., and Indig, F. E. (2003) DNA damage modulates nucleolar interaction of the Werner protein with the AAA ATPase p97/VCP. *Mol. Biol. Cell* **14,** 4221–4229 CrossRef Medline

60. Taylor, J. P. (2015) Multisystem proteinopathy: intersecting genetics in muscle, bone, and brain degeneration. *Neurology* **85,** 658–660 CrossRef Medline
61. Johnson, J. O., Mandrioli, J., Benatar, M., Abramzon, Y., Van Deerlin, V. M., Trojanowski, J. Q., Gibbs, J. R., Brunetti, M., Gronka, S., Wuu, J., Ding, J., McCluskey, L., Martinez-Lage, M., Falcone, D., Hernandez, D. G., *et al.* (2010) Exome sequencing reveals VCP mutations as a cause of familial ALS. *Neuron* **68,** 857–864 CrossRef Medline
62. Kimonis, V. E., Fulchiero, E., Vesa, J., and Watts, G. (2008) VCP disease associated with myopathy, Paget disease of bone and frontotemporal dementia: review of a unique disorder. *Biochim. Biophys. Acta* **1782,** 744–748 CrossRef Medline
63. Mehta, S. G., Khare, M., Ramani, R., Watts, G. D., Simon, M., Osann, K. E., Donkervoort, S., Dec, E., Nalbandian, A., Platt, J., Pasquali, M., Wang, A., Mozaffar, T., Smith, C. D., and Kimonis, V. E. (2013) Genotype-phenotype studies of VCP-associated inclusion body myopathy with Paget disease of bone and/or frontotemporal dementia. *Clin. Genet.* **83,** 422–431 CrossRef Medline
64. Zhou, N., Ma, B., Stoll, S., Hays, T. T., and Qiu, H. (2017) The valosin-containing protein is a novel repressor of cardiomyocyte hypertrophy induced by pressure overload. *Aging Cell* **16,** 1168–1179 CrossRef Medline
65. Vandermoere, F., El Yazidi-Belkoura, I., Slomianny, C., Demont, Y., Bidaux, G., Adriaenssens, E., Lemoine, J., and Hondermarck, H. (2006) The valosin-containing protein (VCP) is a target of Akt signaling required for cell survival. *J. Biol. Chem.* **281,** 14307–14313 CrossRef Medline
66. Song, C., Wang, Q., and Li, C. C. (2003) ATPase activity of p97-valosin-containing protein (VCP). D2 mediates the major enzyme activity, and D1 contributes to the heat-induced activity. *J. Biol. Chem.* **278,** 3648–3655 CrossRef Medline
67. Wang, Q., Song, C., and Li, C. C. (2004) Molecular perspectives on p97-VCP: progress in understanding its structure and diverse biological functions. *J. Struct. Biol.* **146,** 44–57 CrossRef Medline
68. Song, C., Wang, Q., Song, C., Lockett, S. J., Colburn, N. H., Li, C. C., Wang, J. M., and Rogers, T. J. (2015) Nucleocytoplasmic shuttling of valosin-containing protein (VCP/p97) regulated by its N domain and C-terminal region. *Biochim. Biophys. Acta* **1853,** 222–232 CrossRef Medline
69. Matsubara, S., Shimizu, T., Komori, T., Mori-Yoshimura, M., Minami, N., and Hayashi, Y. K. (2016) Nuclear inclusions mimicking poly(A)-binding protein nuclear 1 inclusions in a case of inclusion body myopathy associated with Paget disease of bone and frontotemporal dementia with a novel mutation in the valosin-containing protein gene. *Neuromuscul. Disord.* **26,** 436–440 CrossRef Medline
70. Fatkin, D., MacRae, C., Sasaki, T., Wolff, M. R., Porcu, M., Frenneaux, M., Atherton, J., Vidaillet, H. J., Jr., Spudich, S., De Girolami, U., Seidman, J. G., Seidman, C., Muntoni, F., Müehle, G., Johnson, W., and McDonough, B. (1999) Missense mutations in the rod domain of the lamin A/C gene as causes of dilated cardiomyopathy and conduction-system disease. *N. Engl. J. Med.* **341,** 1715–1724 CrossRef Medline
71. Brody, M. J., Schips, T. G., Vanhoutte, D., Kanisicak, O., Karch, J., Maliken, B. D., Blair, N. S., Sargent, M. A., Prasad, V., and Molkentin, J. D. (2016) Dissection of thrombospondin-4 domains involved in intracellular adaptive ER Stress responsive signaling. *Mol. Cell Biol.* **36,** 2–12 Medline
72. Brody, M. J., Vanhoutte, D., Schips, T. G., Boyer, J. G., Bakshi, C. V., Sargent, M. A., York, A. J., and Molkentin, J. D. (2018) Defective flux of thrombospondin-4 through the secretory pathway impairs cardiomyocyte membrane stability and causes cardiomyopathy. *Mol. Cell Biol.* **38,** e00114-18 Medline
73. Brody, M. J., Feng, L., Grimes, A. C., Hacker, T. A., Olson, T. M., Kamp, T. J., Balijepalli, R. C., and Lee, Y. (2016) LRRC10 is required to maintain cardiac function in response to pressure overload. *Am. J. Physiol. Heart. Circ. Physiol.* **310,** H269–H278 CrossRef Medline
74. Kim, H. J., Kim, N. C., Wang, Y. D., Scarborough, E. A., Moore, J., Diaz, Z., MacLea, K. S., Freibaum, B., Li, S., Molliex, A., Kanagaraj, A. P., Carter, R., Boylan, K. B., Wojtas, A. M., Rademakers, R., *et al.* (2013) Mutations in prion-like domains in hnRNPA2B1 and hnRNPA1 cause multisystem proteinopathy and ALS. *Nature* **495,** 467–473 CrossRef Medline
75. Brody, M. J., Cho, E., Mysliwiec, M. R., Kim, T. G., Carlson, C. D., Lee, K. H., and Lee, Y. (2013) Lrrc10 is a novel cardiac-specific target gene of Nkx2–5 and GATA4. *J. Mol. Cell Cardiol.* **62,** 237–246 CrossRef Medline
76. Brody, M. J., Hacker, T. A., Patel, J. R., Feng, L., Sadoshima, J., Tevosian, S. G., Balijepalli, R. C., Moss, R. L., and Lee, Y. (2012) Ablation of the cardiac-specific gene leucine-rich repeat containing 10 (lrrc10) results in dilated cardiomyopathy. *PLoS ONE* **7,** e51621 CrossRef Medline
77. Quan, H., Fan, Q., Li, C., Wang, Y. Y., and Wang, L. (2018) The transcriptional profiles and functional implications of long non-coding RNAs in the unfolded protein response. *Sci. Rep.* **8,** 4981 CrossRef Medline
78. Paredes, F., Parra, V., Torrealba, N., Navarro-Marquez, M., Gatica, D., Bravo-Sagua, R., Troncoso, R., Pennanen, C., Quiroga, C., Chiong, M., Caesar, C., Taylor, W. R., Molgó, J., San Martin, A., Jaimovich, E., and Lavandero, S. (2016) HERPUD1 protects against oxidative stress-induced apoptosis through down-regulation of the inositol 1,4,5-trisphosphate receptor. *Free Radic. Biol. Med.* **90,** 206–218 CrossRef Medline